COMMUN. MATH. SCI.
Vol. 6, No. 2, pp. 309–329

THE WILLMORE FUNCTIONAL AND INSTABILITIES IN THE CAHN-HILLIARD EQUATION*

MARTIN BURGER†, SHUN-YIN CHU‡, PETER A. MARKOWICH§, AND CAROLA-BIBIANE SCHÖNLIEB¶

Abstract. In this paper we are interested in the finite-time stability of transition solutions of the Cahn-Hilliard equation and its connection to the Willmore functional. We show that the Willmore functional locally decreases or increases in time in the linearly stable or unstable case respectively. This linear analysis explains the behavior near stationary solutions of the Cahn-Hilliard equation. We perform numerical examples in one and two dimensions and show that in the neighbourhood of transition solutions local instabilities occur in finite time. We also show convergence of solutions of the Cahn-Hilliard equation for arbitrary dimension to a stationary state by proving asymptotic decay of the Willmore functional in time.

Key words. Cahn-Hilliard equation, transition solutions, Willmore functional, asymptotics, stability

AMS subject classifications. 35B35, 35K57

1. Introduction

We consider the Neumann problem for the Cahn-Hilliard equation

$$\begin{cases} u_t = \Delta(-\epsilon^2\Delta u + F'(u)), & x\in\Omega, \\ \frac{\partial u}{\partial n} = \frac{\partial}{\partial n}(-\epsilon^2\Delta u + F'(u)) = 0, & x\in\partial\Omega \end{cases} \tag{1.1}$$

with $\Omega\subseteq\mathbb{R}^d$ a bounded domain and $d\geq 1$, though we shall focus primarily on the cases $d=1$ and 2. F is a double well potential with $F'(u)=\frac{1}{2}(u^3-u)$ and $0<\epsilon<<1$ is a small parameter. Note that the function F' is of bistable type. Considering only constant solutions $u=c$ of (1.1), these are classified in the following way. If $F''(u)<0$ then u corresponds to the so called spinodal interval ($|u|<\frac{1}{\sqrt{3}}$) and it is an unstable stationary state. Otherwise u corresponds to the metastable intervals (i.e. $u\in(-1,-\frac{1}{\sqrt{3}})$ or $u\in(\frac{1}{\sqrt{3}},1)$) and is asymptotically stable, see [18] for a detailed description. The Cahn-Hilliard equation is a classic model for phase separation and subsequent phase coarsening of binary alloys. There the solution $u(x,t)$ represents the concentration of one of the two metallic components of the alloy. For further information about the physical background of the Cahn-Hilliard equation we refer, for instance, to [9, 28, 29, 23]. Numerical studies about the behavior of solutions of (1.1) can be found, e.g., in [14, 17], or [26]. Solutions of (1.1) have a time-conserved mean value

$$\int_\Omega u(x,t)dx = \int_\Omega u(x,t=0)dx, \text{ for all } t>0. \tag{1.2}$$

*Received: November 16, 2007; accepted (in revised version: February 23, 2008). Communicated by Markos Katsoulakis.

†Institut für Numerische und Angewandte Mathematik, Fachbereich Mathematik und Informatik, Westfaelische Wilhelms Universitaet (WWU) Muenster, Einsteinstrasse 62, D 48149 Muenster, Germany (martin.burger@uni-muenster.de).

‡RICAM, Austrian Academy of Sciences, Altenbergerstraße 69, A-4040, Linz, Austria (shun-yin.chu@oeaw.ac.at).

§DAMTP, Centre for Mathematical Sciences, Wilberforce Road, Cambridge CB3 0WA, United Kingdom (P.A.Markowich@damtp.cam.ac.uk).

¶DAMTP, Centre for Mathematical Sciences, Wilberforce Road, Cambridge CB3 0WA, United Kingdom (C.B.Schonlieb@damtp.cam.ac.uk).

A way of deriving equation (1.1) has been suggested by Fife in [18]. One takes the Ginzburg-Landau free energy

$$E[u](t) = \int_\Omega \left(\frac{\epsilon^2}{2} |\nabla u(x,t)|^2 + F(u(x,t)) \right) dx \tag{1.3}$$

and looks for constrained (mass-conserving) gradient flows of this functional. The Cahn-Hilliard Equation (1.1) is obtained by taking the gradient flow of (1.3) in the sense of the $H^{-1}(\Omega)$ inner product. The mass constraint is a consequence of the natural boundary conditions for (1.1).

Using the ideas of [24] it is not hard to see that the Cahn-Hilliard equation possesses a global attractor. Zheng proved in [39] convergence to equilibria for solutions of (1.1) in two and three dimensions. In [32] the authors proved that solutions of the Cahn-Hilliard equation converge to equilibria in dimensions $d = 1, 2$ and 3. In one space dimension the equilibria are isolated [27] and the global attractor is finite-dimensional. Further, Grinfeld and Novick-Cohen give a full description of the stationary solutions of the viscous Cahn-Hilliard equation in one space dimension; compare [21, 22]. So far equilibria have been determined and their properties studied only in the one dimensional case. It is a major problem to characterize the equilibria in more than one dimension. The reason is that the limit set of the solutions can be large. However, some papers such as [35, 36, 37, 19, 12] still provide certain special types of equilibrium solutions. A special type of stationary solution of (1.1) is the so-called transition solution, which continuously connects the two stable equilibria, -1 and 1. In one dimension the so called kink solution $u_0 = \tanh \frac{x}{2\epsilon}$ is such a stationary solution of the Cahn-Hilliard equation. The radially-symmetric analogue in two dimensions are the so called bubble solutions. In [8] asymptotic stability was shown for the kink solution for fixed $\epsilon = 1$, i.e., small perturbations of u_0 in some suitable norm will decay to zero in time. Further studies for the one-dimensional case describe the motion of transition layers; compare [1, 7, 3, 20]. In [2] Alikakos and Fusco proved spectral estimates of the linearized fourth order Cahn-Hilliard operator in two dimensions near bubble solutions. Some of their results are discussed later in Section 3.

In this paper we investigate the stability of transition solutions of the Cahn-Hilliard equation in finite time and its connection to the Willmore functional. The backward second-order diffusion (for $|u| < \frac{1}{\sqrt{3}}$) in the equation gradually affects the solution, which can result in phenomena like local instabilities or oscillating patterns, controlled by the fourth-order term on scales of order ϵ. We are going to show that in the neighbourhood of transition solutions small instabilities occur in finite time. In general it is natural to study stationary solutions of the Cahn-Hilliard equation by analyzing the energy functional (1.3). The energy functional decreases in time since

$$\frac{d}{dt} E[u](t) + \int_\Omega |\nabla(-\epsilon^2 \Delta u(x,t) + F'(u(x,t)))|^2 \, dx = 0. \tag{1.4}$$

Because of this monotonicity the energy functional is not suitable for the study of local (in space and time) behavior of the Cahn-Hilliard equation. Instead we present analytical and numerical evidence that the numerically observed instabilities are connected with the evolution of the Willmore functional. The Willmore functional of the Cahn-Hilliard Equation (1.1) is given by

$$W[u](t) = \frac{1}{4\epsilon} \int_\Omega (\epsilon \Delta u(x,t) - \frac{1}{\epsilon} F'(u(x,t)))^2 dx, \tag{1.5}$$

and is considered to describe the geometric boundary of two different stable states and the movement of curves under anisotropic flows. It has its origin in differential geometry where it appears as a phase field approximation for solutions of the so called Willmore problem (cf. [38]). The Willmore problem is to find a surface Γ in an admissible class embedded in $\mathbb{R}^3$ which minimizes the mean curvature energy $\int_\Gamma H^2\,dS$ under certain constraints on the surface, where $H=(\kappa_1+\kappa_2)/2$ is the mean curvature and κ_1,κ_2 are the principal curvatures of Γ. For the analytical and computational modelling of a minimizing surface of the Willmore problem the phase field method is considered among other approaches. In [13] the authors consider solutions of a constrained minimization problem for (1.5) of the form $u_\epsilon(x)=\tanh\frac{d(x)}{\sqrt{2}\epsilon}+\epsilon h$ with fixed mass and fixed energy (1.3), where d is the signed distance function to the zero level set of u_ϵ and h is an arbitrary function in $C^2(\Omega)$ independent of ϵ. They show that the level sets $\{u_\epsilon=0\}$ converge uniformly to a critical point of the Willmore problem as $\epsilon\to 0$. Also in this range of considerations falls a modified De Giorgi conjecture. The authors of [30] considered functionals $F_\epsilon: L^1(\Omega)\to\mathbb{R}$ for domains $\Omega\in\mathbb{R}^2$ and $\mathbb{R}^3$ with

$$F_\epsilon[u](t)=E[u](t)+4W[u](t)$$

if $u\in L^1(\Omega)\cap W^{2,2}(\Omega)$ and $F_\epsilon[u](t)=\infty$ if $u\in L^1(\Omega)\setminus W^{2,2}(\Omega)$. They showed that this sequence of functionals evaluated in characteristic functions $\chi=2\chi_E-1$, with $E\subset\Omega$ a subset, $\Gamma-$ converges in $L^1(\Omega)$ as $\epsilon\to 0$ to a functional $F[\chi]$ given by

$$F[\chi](t)=\sigma\mathcal{H}^{n-1}(\partial E\cap\Omega)+\sigma\int_{\partial E\cap\Omega}|\mathbf{H}_{\partial E}|^2\,d\mathcal{H}^{n-1}.$$

Here $\sigma=\int_{-1}^1\sqrt{2F}$ (where F is the double well potential), $\mathbf{H}_{\partial E}$ denotes the mean curvature vector of ∂E and $\mathcal{H}^{n-1}$ is the $n-1$ dimensional Hausdorff measure. This result indicates that possible instabilities of (1.1) disappear for the limit $\epsilon\to 0$. We will encounter this observation again in our numerical examples for small values of ϵ. For additional considerations of $\Gamma-$ limits of this type see [31] and especially [11]. In the following we use the Willmore functional to detect local instabilities in finite time of transition solutions of (1.1) for small values of $\epsilon<<1$. As said above, in one space dimension they are given by the kink solutions of the form $\tanh\frac{d(x)}{\sqrt{2}\epsilon}$. In two dimensions we consider their radially-symmetric analogues called bubble solutions.

To get an insight into the behavior of the Willmore functional for solutions of (1.1) we start with an asymptotic analysis. In Section 2 we study the asymptotic limit of solutions of the Cahn-Hilliard equation for arbitrary space dimension $d\geq 1$ by showing asymptotic decay of the Willmore functional in time. The main challenge of the proof of convergence in this paper is that we avoid using the Lojasiewicz inequality as before, say in [32]. It was shown in [25] that gradient flows in $\mathbb{R}^d$ (and even in L^2, compare [33]) fulfill the Lojasiewicz inequality, which implies convergence to equilibrium of solutions of the gradient system. For the application to the Cahn-Hilliard equation it takes a serious effort to prove validity of the Lojasiewicz inequality for gradient flows in H^{-1}, as proved in [32]. We circumvent this difficulty and prove the following Theorem.

THEOREM 1.1. *Let u be the solution of the Cahn-Hilliard equation with initial data $u^0 = u^0(x)$, either posed as a Cauchy problem in $\Omega = \mathbb{R}^d$, $d \geq 1$, or in a bounded domain Ω with Neumann boundary conditions. We assume*

$$\int_\Omega F'(u)dx = 0 \text{ for all } t > 0. \tag{1.6}$$

For $\Omega = \mathbb{R}^n$ further suppose

$$\begin{cases} \epsilon^2 \Delta u^0 - F'(u^0) \text{ and } \nabla(\epsilon^2 \Delta u^0 - F'(u^0)) \text{ are} \\ \text{spatially exponentially decaying as } |x| \to \infty. \end{cases} \tag{1.7}$$

Then it follows that

$$\lim_{t \to \infty} W[u](t) = 0.$$

REMARK 1.2.

- *Note that the Assumption (1.6) in Theorem 1.1 is no restriction on F. Since $\int_\Omega F'(u)dx$ is a constant, we can rewrite the equation as*

$$\begin{aligned} u_t &= \Delta(-\epsilon^2 \Delta u + F'(u) - \frac{1}{|\Omega|} \int_\Omega F'(u)dx) \\ &= \Delta(-\epsilon^2 \Delta u + \tilde{f}(u)), \end{aligned}$$

  with $\int_\Omega \tilde{f}(u)dx = 0$ where $\tilde{f}(u)$ is equal to $F'(u)$ shifted by the constant $\frac{1}{|\Omega|}\int_\Omega F'(u)dx$. In the case of Neumann boundary conditions it further follows from (1.1) that

$$\frac{\partial u}{\partial n} = \frac{\partial(-\epsilon^2 \Delta u + \tilde{f}(u))}{\partial n} = 0.$$

  Thus shifting $F'(u)$ by a constant does not change the equation and Assumption (1.6) is reasonable.
- *Note that condition (1.7) extends its validity from the initial conditions u^0 to $u(.,t)$ for arbitrary times $t > 0$ due to the mass conservation (1.2) of solutions of (1.1).*

The challenge of proving convergence of the Willmore functional is that it is generally not monotone in time. To overcome this we construct a nonnegative functional balancing the Willmore functional with the energy functional so that the strong decay property of the energy takes the main role controlling increasing parts appearing in the Willmore functional.

The next step is to analyze the behavior of the Willmore functional and its connection to the behavior of solutions of (1.1) in finite time. For this sake we consider the linearized Cahn-Hilliard equation. In fact the behavior of solutions of the nonlinear equation is similar in the neighbourhood of stationary solutions to that of the linear equation. Sander and Wanner discussed in [34] that solutions of (1.1) which start near a homogeneous equilibrium within the spinodal interval remain close to the corresponding solution of the linearized equation with high probability (depending on how likely it is to find an appropriate initial condition) for an unexpectedly long time. In particular we are interested in instabilities that appear both locally in time and space. To motivate this better let us consider the Cahn-Hilliard equation near a constant equilibrium state $\tilde{u}$ on the whole space $\Omega = \mathbb{R}^d$. Set $u = \tilde{u} + \delta v$, $\delta \in \mathbb{R}$ small; then the perturbation v fulfills in first approximation

$$\begin{aligned} &v_t = -\epsilon^2 \Delta^2 v + a\Delta v && \text{in } \mathbb{R}^d, t > 0, \\ &v(t=0) = v_0(x) && \text{in } \mathbb{R}^d, \end{aligned}$$

with $a = F''(\tilde{u}) = \frac{1}{2}(3\tilde{u}^2 - 1)$. The above equation reads after Fourier transform

$$\begin{aligned} &\hat{v}_t(\xi,t) = (-\epsilon^2 |\xi|^4 - a|\xi|^2)\hat{v}, && \xi \in \mathbb{R}^d, t > 0, \\ &\hat{v}(t=0) = \hat{v_0}(\xi), && \xi \in \mathbb{R}^d. \end{aligned}$$

This equation can be explicitly solved:

$$\hat{v}(\xi,t) = \exp(-|\xi|^2 (\epsilon^2 |\xi|^2 + a)t)\hat{v_0}(\xi).$$

If $a = F''(\tilde{u}) < 0$ (this means that $\tilde{u}$ lies in the spinodal interval $(-1/\sqrt{3}, 1/\sqrt{3})$) then $\hat{v}(\xi,t) \to \infty$ for $\xi \in \left\{ |\xi| < \sqrt{|a|}/\epsilon \right\} \cap \operatorname{supp}\hat{v_0}$, i.e., frequencies less than $\sqrt{|a|}/\epsilon$ become amplified if they are present in the initial datum. In our case we consider solutions in the neighbourhood of transition solutions, i.e. transition solutions perturbed where they assume values from the spinodal interval. Referring again to [30], the linear instability explained above is also valid for the nonlinear Cahn-Hilliard equation for a finite time until the effect of the nonlinearity becomes strong enough to stabilize the solution again. This results in instabilities local in space and time. In Section 3, spectral estimates for transition solutions tracing back to Alikakos, Bates and Fusco (cf. [1, 2]) are presented for one and two dimensions. Further, the important role of the Willmore functional for finite-time stability/instability analysis for the Cahn-Hilliard equation is motivated. For ϵ fixed we linearize the Willmore functional at a stationary solution of the Cahn-Hilliard Equation (1.1) perturbed by an eigenvector of the linearized Cahn-Hilliard operator. We show that the Willmore functional decreases in time for eigenvectors corresponding to a negative eigenvalue and increases in the case of a positive eigenvalue. In other words,

$$\begin{aligned} &\frac{d}{dt} W[v](t) \leq 0 \iff \lambda < 0 \iff \text{ linearly stable}, \\ &\frac{d}{dt} W[v](t) \geq 0 \iff \lambda > 0 \iff \text{ linearly unstable}, \end{aligned}$$

where $v = \tilde{u} + \delta v_0$, with $\tilde{u}$ a stationary solution of (1.1) and v_0 the eigenvector to the eigenvalue λ of the linearized equation. Roughly said, this means that linear instabilities — which correspond to positive eigenvalues of the Cahn-Hilliard equation — can be detected by considering the evolution of the Willmore functional.

In Section 4 we perform numerical computations for (1.1) near transition solutions in one and two dimensions. We remark that in the past 20 years numerical approximations of the solutions of the Cahn-Hilliard equation — for purposes different from ours — have been studied by many authors, see [16] and [17] for further references. We use a semi-implicit approximation in time and finite elements for the space discretization in this paper. We start the computation at $t = 0$ with a transition solution perturbed within its transition area with values from the spinodal interval of the equation. Motivated by the linear stability analysis of Section 3 we discuss stability in terms of the Willmore functional. We say a function $u(x,t)$ shows an unstable behavior at time $0<t_0<\infty$ if

$$\frac{d}{dt}W[u](t_0)>0.$$

Conversely, we say the function $u(x,t)$ is stable for all times $0<t<t_0$ if

$$\frac{d}{dt}W[u](t)\leq 0.$$

Organization of the paper. In Section 2 we prove Theorem 1.1. The linear analysis of the Willmore functional is given in Section 3. Finally, in Section 4 we perform numerical computations for the Cahn-Hilliard Equation (1.1) near transition solutions in dimensions 1 and 2.

2. Proof of Theorem 1.1

In this section we present the proof of Theorem 1.1, which will be split into various lemmas and propositions. In the following the long time asymptotic behavior of solutions of the Cahn-Hilliard equation is studied by exploring the Willmore functional. We consider the d-dimensional case of the Cahn-Hilliard equation. All following arguments hold true both for the Neumann boundary problem and the Cauchy problem in $\mathbb{R}^d$ with certain conditions on the spatial decay of the solutions. We start by introducing some useful properties of the functionals in our setting of the stationary profile.

Lemma 2.1. *Let u be the solution of the Cahn-Hilliard equation as posed in Theorem 1.1. Then for any test function $\phi=\phi(x,t)\in C_0^\infty(\Omega\times(0,\infty))$ we have*

$$\begin{aligned}
&\frac{d}{dt}\int_\Omega \phi\left(\frac{\epsilon^2}{2}|\nabla u|^2+F(u)\right)dx+\int_\Omega \phi|\nabla(\epsilon^2\Delta u-F'(u))|^2\,dx\\
=&\int_\Omega \phi_t\left(\frac{\epsilon^2}{2}|\nabla u|^2+F(u)\right)dx+\frac{1}{2}\int_\Omega \Delta\phi(F'(u)-\epsilon^2\Delta u)^2dx\\
&-\epsilon^2\int_\Omega \nabla(\nabla\phi\cdot\nabla u)\cdot\nabla(\epsilon^2\Delta u-F'(u))\,dx.
\end{aligned}$$

Lemma 2.2. *Let u be the solution of the Cahn-Hilliard equation as posed in Theorem 1.1. Then we have*

$$\begin{aligned}
&\frac{d}{dt}\int_\Omega(\epsilon\Delta u-\frac{1}{\epsilon}F'(u))^2dx+2\epsilon^2\int_\Omega|\Delta(\epsilon\Delta u-\frac{1}{\epsilon}F'(u))|^2dx\\
=&2\int_\Omega F''(u)(\epsilon\Delta u-\frac{1}{\epsilon}F'(u))\Delta(\epsilon\Delta u-\frac{1}{\epsilon}F'(u))dx,
\end{aligned}$$

and

$$\begin{aligned}
&\frac{d}{dt}\int_\Omega(\Delta(\epsilon\Delta u-\frac{1}{\epsilon}F'(u)))^2dx+2\epsilon^2\int_\Omega(\Delta^2(\epsilon\Delta u-\frac{1}{\epsilon}F'(u)))^2dx\\
=&2\int_\Omega F''(u)\Delta(\epsilon\Delta u-\frac{1}{\epsilon}F'(u))\Delta^2(\epsilon\Delta u-\frac{1}{\epsilon}F'(u))dx.
\end{aligned}$$

The proofs of Lemma 2.1 and 2.2 are straightforward. Note that both lemmas hold for Ω a bounded domain as well as Ω unbounded provided condition (1.7) from Theorem 1.1 holds.

Proposition 2.3. *Let $f,g\in C^1([0,\infty))$ be nonnegative functions with $g'(t)\leq 0$ everywhere,* $\mathrm{supp} f\subset \mathrm{supp} g$, $\sup_{t\in \mathrm{supp} g}\frac{f}{g}$ *and* $\sup_{t\in\mathrm{supp} g}\frac{(f')^+}{g}$ *bounded, where* $(f')^+(t)=\max\{f'(t),0\}$. *Under the same assumptions as in Theorem 1.1 and for a sufficiently large constant C we have*

$$\frac{d}{dt}\Big[\int_\Omega f(t)(\epsilon\Delta u-\frac{1}{\epsilon}F'(u))^2dx+\frac{C}{\epsilon^2}\int_\Omega g(t)\left(\frac{\epsilon^2}{2}|\nabla u|^2+F(u)\right)dx\Big]\leq 0.$$

In particular, $\epsilon^3 W[u](t)+CE[u](t)\leq \epsilon^3 W[u^0]+CE[u^0]$.

Proof. Consider the functional

$$U[u](t)=\int f(t)(\epsilon\Delta u-\frac{1}{\epsilon}F'(u))^2dx+\frac{C}{\epsilon^2}\int g(t)\left(\frac{\epsilon^2}{2}|\nabla u|^2+F(u)\right)dx.$$

By using the identity in Lemma 2.2 for the first term in $U[u](t)$ and Lemma 2.1 for the second term, we derive

$$\begin{aligned}\frac{d}{dt}U[u](t)=&f'(t)\int(\epsilon\Delta u-\frac{1}{\epsilon}F'(u))^2dx+\frac{C}{\epsilon^2}g'(t)\int\frac{\epsilon^2}{2}|\nabla u|^2+F(u)dx\\&+f(t)\Big[2\int F''(u)(\epsilon\Delta u-\frac{1}{\epsilon}F'(u))\Delta(\epsilon\Delta u-\frac{1}{\epsilon}F'(u))dx\\&-2\epsilon^2\int|\Delta(\epsilon\Delta u-\frac{1}{\epsilon}F'(u))|^2dx\Big]-\frac{C}{\epsilon^2}g(t)\int|\nabla(-\epsilon^2\Delta u+F'(u))|^2dx.\end{aligned}\tag{2.1}$$

For the case $\Omega=\mathbb{R}^d$ we need the following lemma to deal with the last term in (2.1).

Lemma 2.4 (modified Poincare inequality on $\mathbb{R}^d$). *Let $a>0,C_1>0,C_2>0$ be fixed constants. Then there exists a positive constant $C_0=C_0(a,C_1,C_2)$ such that for any functions f in*

$$\begin{aligned}V_{a,C_1,C_2}=\{f\in H^1(\mathbb{R}^d):\int_{\mathbb{R}^d}f\,dx=0,|f(x)|\leq C_1e^{-a|x|}|f|_{L^2},\\|f'(x)|\leq C_2e^{-a|x|}|f|_{L^2}\text{ for }x\in\mathbb{R}^d\},\end{aligned}$$

we have

$$|f|_{L^2(\mathbb{R}^d)}\leq C_0|\nabla f|_{L^2(\mathbb{R}^d)}.$$

Taking into account condition (1.7) for the spatial decay of the involved quantities and by using Lemma 2.4 for $\Omega=\mathbb{R}^d$, the right side of (2.1) can be bounded by

$$\begin{aligned}&\left((f'(t))^+-\frac{Cg(t)}{C_0}\right)\int(\epsilon\Delta u-\frac{1}{\epsilon}F'(u))^2dx\\&+2f(t)\sup_{|u|\leq 2}|F''(u)|\int|\epsilon\Delta u-\frac{1}{\epsilon}F'(u)|\cdot|\Delta(\epsilon\Delta u-\frac{1}{\epsilon}F'(u))|dx\\&-2f(t)\epsilon^2\int|\Delta(\epsilon\Delta u-\frac{1}{\epsilon}F'(u))|^2dx+\frac{C}{\epsilon^2}g'(t)E[u](t).\end{aligned}$$

This term is non-positive when C is chosen to be large enough such that

$$f(t)^2 \sup_{|u|\leq 2} |F''(u)|^2 - \Big((f'(t))^+ - \frac{Cg(t)}{C_0}\Big)(-2f(t)\epsilon^2) \leq 0,$$

that is, choosing $C > \frac{C_0 f(t)(\sup_{|u|\leq 2}|F''(u)|)^2}{2\epsilon^2 g(t)} + \frac{C_0(f'(t))^+}{g(t)}$ for $t \in \mathrm{supp} g$. □

REMARK 2.5. *Note that the Poincare inequality on $\mathbb{R}^d$ is not valid in general. Consider for example the function $h_a(x) = a^{\frac{n+2}{2b}} x e^{-a|x|^b}$ with $a>0$ and some fixed $b>0$. Then $\int h_a^2 dx = O(1)$ and $\int h_a'^2 dx = O(a^{\frac{2}{b}})$ as $a \to 0+$. Therefore,*

$$\frac{|h_a'|_{L^2}}{|h_a|_{L^2}} = O(a^{\frac{1}{b}}) \to 0$$

as a tends to zero, which contradicts the Poincare inequality.

Finally we come to the proof of the main result of this section, Theorem 1.1.

Proof. [Proof of Theorem 1.1.]
Step 1: Let

$$f(t) = \begin{cases} \frac{1+t}{2}, & 0 \leq t \leq 1, \\ 2-t, & 1 \leq t \leq 2, \\ 0, & t \geq 2, \end{cases}$$

and

$$g(t) = \begin{cases} 1, & t \leq 2, \\ 0, & t \geq 3. \end{cases}$$

Let C be a fixed constant chosen as in Proposition 2.3. The functional

$$U[u](t) \equiv 4\epsilon f(t) W[u](t) + \frac{C}{\epsilon^2} g(t) E[u](t)$$

is decreasing in time and $U[u](t=1) \leq U[u](t=0)$. That is,

$$W[u](t=1) + \frac{C}{4\epsilon^3} E[u](t=1) \leq \frac{1}{2} W[u](t=0) + \frac{C}{4\epsilon^3} E[u](t=0).$$

Step 2: For each $n \in \mathbb{N}$, setting $f(t-n+1)$ and $g(t-n+1)$ as in Proposition 2.3, we can again find inequalities for $n-1 \leq t \leq n$ and obtain

$$W[u](t=n) + \frac{C}{4\epsilon^3} E[u](t=n) \leq \frac{1}{2} W[u](t=n-1) + \frac{C}{4\epsilon^3} E[u](t=n-1). \tag{2.2}$$

Set $\alpha_n = W[u](t=n)$. Then (2.2) can be rewritten as

$$\alpha_n \leq \frac{1}{2}\alpha_{n-1} + \frac{C}{4\epsilon^3} \int_{n-1}^{n} \int_\Omega |\nabla(-\epsilon^2 \Delta u + F'(u))|^2 dx dt,$$

where we used the decay property (1.4) of the energy functional from Section 1.

Step 3: We want to show that α_n tends to zero as n tends to infinity. By an iterative argument we get

$$\begin{aligned}\alpha_n \leq & \left(\frac{1}{2}\right)^n \alpha_0 \\ & + \frac{C}{4\epsilon^3}\Big(\left(\frac{1}{2}\right)^{n-1}\int_0^1\int_\Omega |\nabla(-\epsilon^2\Delta u + F'(u))|^2 dxdt \\ & + \left(\frac{1}{2}\right)^{n-2}\int_1^2\int_\Omega |\nabla(-\epsilon^2\Delta u + F'(u))|^2 dxdt \\ & + \cdots + \frac{1}{2}\int_{n-2}^{n-1}\int_\Omega |\nabla(-\epsilon^2\Delta u + F'(u))|^2 dxdt \\ & + \int_{n-1}^{n}\int_\Omega |\nabla(-\epsilon^2\Delta u + F'(u))|^2 dxdt\Big).\end{aligned}$$

Using a standard fact from analysis formulated in the following Lemma 2.6, it follows that α_n converges to 0 for $n \to \infty$.

Lemma 2.6. *Let $(a_n),(b_n)$ be two nonnegative sequences such that their sums $\sum_n a_n$ and $\sum_n b_n$ are convergent. Then*

$$\lim_{n\to\infty} \sum_{i=0}^{n} a_i b_{n-i} = 0.$$

We conclude our proof in step 4.

Step 4: It remains to prove that for any sequence (t_n) tending to infinity, $W[u](t_n)$ converges to zero. To do so it suffices to prove that for any fixed integer $q > 0$, $(W[u](t = \frac{n}{q}))_n$ converges to zero. Repeating the computations of Step 3 for the inequality (2.2) for all rational values of t in between $n-1$ and n, the proof is similar and we omit the details here. □

Remark 2.7. *Note that the proof of Theorem 1.1 also trivially provides decay of u_t in H^{-2}, namely,*

$$\begin{aligned}\|u_t\|_{H^{-2}} &= \|\Delta(-\epsilon^2\Delta u + F'(u))\|_{H^{-2}} \\ &\leq C\| - \epsilon^2\Delta u + F'(u)\|_{L^2} \\ &\to 0 \text{ as } t \to \infty.\end{aligned}$$

So we have shown that the Willmore functional asymptotically decreases to zero under the assumptions of Theorem 1.1. This additionally proves that $u_t \to 0$ for $t \to \infty$ in $H^{-2}(\Omega)$ for every $\epsilon > 0$ and arbitrary dimension d.

3. Linear stability / instability

In this section we consider the small time behavior of solutions of the Cahn-Hilliard equation. We relate local-in-time instabilities of solutions with the Willmore functional by comparing the eigenvalues of the linearized operator with the evolution of the Willmore functional. We begin with a short discussion of spectral estimates and conclude with presenting the new result.

For the one dimensional case Alikakos, Bates and Fusco showed in [1] that there is exactly one unstable eigenvalue of the linearized Cahn-Hilliard eigenvalue problem. For simplicity let $D=[0,1]$. They consider the problem linearized at an invariant manifold $\mathcal{M}$ formed by the translation of a self-similar solution $u_\epsilon^\xi(x)=u_\epsilon(x-\xi)\in\mathcal{M}$ with parameter ξ:

$$\begin{cases} -\epsilon^2 H'''' + (F''(u_\epsilon^\xi)H')' = \lambda(\epsilon)H, & 0<x<1, \\ H=H''=0, & x=0,1. \end{cases} \tag{3.1}$$

The first eigenvalue is simple and exponentially small for small $\epsilon>0$:

$$0<\lambda_1^\xi(\epsilon)=O\Big(\frac{(u_{xx}^\xi(0))^2}{\epsilon^3}\Big)=O\Big(\frac{e^{-\frac{2\nu\delta_\xi}{\epsilon}}}{\epsilon^7}\Big), \tag{3.2}$$

where δ_ξ is a small positive constant given in the proof of (3.2) in [1] and ν is a generic constant; see [10]. The remaining spectrum is bounded from above by

$$\lambda_i^\xi(\epsilon)\le -C<0, \quad i=2,3,\dots$$

where C is positive and independent of ϵ,ξ. Both results are contained in [1].

In two dimensions Alikakos and Fusco [2] proved that there is a two-dimensional invariant manifold with exponentially small eigenvalues where the solutions asymptotically develop droplets on the boundary with a speed which is exponentially small. These superslow solutions are called bubble solutions and correspond to an approximate spherical interface drifting slowly towards the boundary, without changing its shape. Solutions like that are typical in the final stages of evolution of (1.1) for general initial conditions. Further, they showed that the dimension of eigenspaces of superslow eigenvalues of the linearized Cahn-Hilliard equation on $D\subseteq\mathbb{R}^d$ is at most d for $d>1$. For simplicity of explanation we consider the eigenvalue problem of the linearized fourth order Cahn-Hilliard operator in $D\subseteq\mathbb{R}^2$. The results in higher dimensions are analogous to this case. Let $U(\eta)$ be the unique increasing bounded solution of $U''-F(U)=0$ on $\mathbb{R}$, and $V(\eta)$ a bounded function that satisfies the orthogonality condition

$$\int_{-\infty}^{\infty} f''(U(\eta))\dot{U}^2(\eta)V(\eta)d\eta=0,$$

where $f(u)=F'(u)$. We consider a one-parameter family of functions $u_\epsilon^\xi(x)$ represented by

$$u_\epsilon^\xi(x)=\begin{cases} U(\frac{x-\rho}{\epsilon})+\epsilon V(\frac{x-\rho}{\epsilon})+O(\epsilon^2), & |y-\rho|\le\lambda, \\ q_\epsilon(x), & |y-\rho|>\lambda, \end{cases}$$

where $y=|x-\xi|$, $\rho>0$ and $q_\epsilon(x)$ is an arbitrary function with $f'(q_\epsilon(x))\ge c>0$. The function $u_\epsilon^\xi(x)$ represents a bubble with center $\xi\in D$ and radius ρ. The eigenvalue problem of the Cahn-Hilliard operator linearized in $u_\epsilon^\xi(x)$, i.e., $L^\xi=\Delta(-\epsilon^2\Delta+F''(u_\epsilon^\xi))$, is given by

$$L^\xi(\phi)=\lambda\phi, \qquad x\in D\subseteq\mathbb{R}^2, \tag{3.3}$$

with Neumann boundary conditions

$$\frac{\partial\phi}{\partial n}=\frac{\partial}{\partial n}(-\epsilon^2\Delta\phi+F''(u_\epsilon^\xi)\phi)=0, \qquad x\in\partial D.$$

In [2] Alikakos and Fusco stated the following result.

Theorem 3.1. *Let $\lambda_1^\epsilon \geq \lambda_2^\epsilon \geq \lambda_3^\epsilon \geq \cdots$ be the eigenvalues of* (3.3)*. Let $\rho > 0, \delta > 0$ be fixed. Then there exists an $\epsilon_0 > 0$ and constants $c, C, C' > 0$, independent of ϵ, such that for $0 < \epsilon < \epsilon_0$ and $\xi \in D$ with $d(\xi, \partial D) > \delta$, the following estimates hold true:*

$$Ce^{-\frac{c}{\epsilon}} \geq \lambda_1^\epsilon \geq \lambda_2^\epsilon \geq -Ce^{-\frac{c}{\epsilon}},$$
$$\lambda_3^\epsilon \leq -C'\epsilon.$$

The first two eigenvalues $\lambda_1^\epsilon, \lambda_2^\epsilon$ are superslow and the others are negative.

Now we present the connection between linear stability properties of the Cahn-Hilliard equation and the Willmore functional. In the following we provide a linear stability analysis around an equilibrium state u_0 satisfying

$$-\epsilon^2 \Delta u_0 + F'(u_0) = 0.$$

More precisely, we look for a solution of the form

$$u(x,t) = u_0(x) + \delta v(x,t) + \mathcal{O}(\delta^2)$$

for sufficiently small $0 < \delta \ll 1$ and some perturbation $v(x,t)$. Due to mass conservation we assume that v has mean zero for all times,

$$\int_\Omega v(x,t)dx = 0 \quad \forall t > 0.$$

We obtain the first-order evolution with respect to δ via the linearized equation

$$v_t = \Delta(-\epsilon^2 \Delta v + F''(u_0)v) := \Delta L_0 v. \tag{3.4}$$

We now compute the asymptotic expansion of the Willmore functional as $\delta \to 0$. It can be expanded as

$$W[u] = W[u_0] + \delta W'[u_0]v + \frac{\delta^2}{2} W''[u_0](v,v) + \mathcal{O}(\delta^3), \tag{3.5}$$

where the first and second order derivatives are taken as variations

$$W'[u_0]v = \int (-\epsilon^2 \Delta u_0 + F'(u_0))(-\epsilon^2 \Delta v + F''(u_0)v)dx$$

and

$$W''[u_0](v,w) = \int (L_0 v)(L_0 w)dx + \int (-\epsilon^2 \Delta u_0 + F'(u_0))F'''(u_0)vw dx.$$

Since u_0 is a stationary solution, we have

$$W'[u_0]v = 0 \ \text{ and } \ W''[u_0](v,v) = \int (L_0 v)^2 dx.$$

Now let v_0 be an eigenfunction of the linearized fourth-order Cahn-Hilliard operator, i.e., there is $\lambda \neq 0$ such that

$$\Delta(L_0 v_0) = \lambda v_0,$$

with Neumann boundary condition $\frac{\partial v_0}{\partial n}|_{\partial\Omega}=0$ and a mean v_0 of zero. Note that λ is real, since v_0 solves a symmetric eigenvalue problem in the scalar product of H^{-1}, defined here as the dual of $H^1(\Omega)\cap\{u:\int_\Omega u\,dx=0\}$. The standard linear stability analysis yields that the perturbation of u_0 by δv_0 is linearly stable for $\lambda<0$ and unstable for $\lambda>0$. These two cases can be translated directly into the local-in-time behavior of the Willmore functional, whose time derivative at time $t=0$ is given by

$$\begin{aligned}\frac{d}{dt}W[u(t)]|_{t=0} &= \delta W'[u_0]v_t|_{t=0}+\delta^2 W''[u_0](v,v_t)|_{t=0}+\mathcal{O}(\delta^3)\\ &= \delta^2\int (L_0v_0)(L_0v_t)dx+\mathcal{O}(\delta^3)\\ &= \delta^2\int (L_0v_0)(L_0\Delta L_0v_0)dx+\mathcal{O}(\delta^3)\\ &= \delta^2\int (L_0v_0)(L_0(\lambda v_0))dx+\mathcal{O}(\delta^3)\\ &= \lambda\delta^2\int (L_0v)^2dx+\mathcal{O}(\delta^3).\end{aligned}$$

This means that, to leading order, the time derivative of $W[u]$ has the same sign as λ, i.e., the Willmore functional is locally increasing in time in the unstable case and locally decreasing in the stable case.

4. Nonlinear stability / instability

We expect the behavior of solutions of the nonlinear Equation (1.1) to be dominated by the behavior of the linear equation in the neighbourhood of stationary solutions; compare Section 1. Therefore, numerical examples may very well give us a good idea about the behavior of solutions and their connection to the Willmore functional even for the nonlinear case. In the following a semi-implicit finite element discretization for the Cahn-Hilliard equation is briefly described and numerical examples are discussed.

4.1. Numerical Discretization. To discretize a fourth-order equation with boundary conditions as above it is often convenient to write it as a system of two equations of second order. In our case of the Cahn-Hilliard equation this results in the following system:

$$\begin{aligned}&u_t=\Delta v\\ &v=-\epsilon^2\Delta u+F'(u),\end{aligned}$$

with Neumann boundary conditions

$$\frac{\partial u}{\partial n}=\frac{\partial v}{\partial n}=0, x\in\partial\Omega.$$

The following issues have to be taken into consideration.

- Explicit schemes for fourth order equations restrict time steps to be of order $O(h^4)$, where h is the spatial grid size.
- Fully implicit schemes are unconditionally stable. The disadvantage is the high computational effort for solving nonlinear equations.
- Semi-implicit schemes are a compromise between explicit and implicit discretization. Shortly said, semi-implicit means that the equation is split into

a convex and a concave part and discretized implicitly and explicitly, respectively; see ([6], [15]). Therefore, the restriction on the step sizes is less severe, and we do not have to solve nonlinear equations.

For these reasons we use the following semi-implicit approximation:

$$\begin{aligned}\frac{u(t,x)-u(t-\Delta t,x)}{\Delta t} &= \Delta v(t,x)\\ v(t,x) &= -\epsilon^2\Delta u(t,x)+F'(u(t-\Delta t,x))\\ &\quad +F''(u(t-\Delta t,x))\cdot(u(t,x)-u(t-\Delta t,x)).\end{aligned}$$

Note that F' is Taylor-expanded at the solution of the previous time step $u(t-\Delta t)$. For the space discretization we use linear finite elements on an equidistant grid in one dimension and on a rectangular grid in two dimensions.

4.2. Numerical examples. In the following examples we consider the solution of the Cahn-Hilliard equation in one and two dimensions for different initial states in a neighbourhood of a transition solution. In the one dimensional case the so called kink solution is given by $u_0(x)=\tanh(\frac{x}{2\epsilon})$. As a first approach in the one dimensional analysis we take as initial value $u(x,t=0)=u_0(x)+p(x)$. The function p denotes a particular kind of zero-mean perturbation, namely

$$p(x)=\begin{cases} a\cdot\sin(f\pi\frac{x}{C\epsilon}) & x\in(-C\cdot\epsilon,C\cdot\epsilon)\\ 0 & \text{otherwise,}\end{cases}$$

with amplitude $a>0$, frequency $f>0$ and support $(-C\cdot\epsilon,C\cdot\epsilon)$ with $C>0$. The amplitude a is chosen such that values of u within the support of the perturbation lie in the spinodal interval of the equation (which is the back diffusion interval).

Varying the parameter ϵ and the support, the amplitude and the frequency of p, we want to observe how the solutions evolve in time. The behavior of the solutions is further compared with the evolution of the corresponding energy functional and the Willmore functional.

We begin with a fixed $\epsilon=0.1$. For the first two examples in Figure 4.1 and 4.2 a fixed step size in space and time discretization was used. For spatial step size we took $\Delta x=0.05\cdot\epsilon$ and for the timesteps $\Delta t=10^3\cdot\epsilon$. The parameters amplitude and frequency of the perturbation are also fixed to 1. The difference between the two examples is the support of the perturbation; on which the convergence process depends.

In the first example an unstable state occurs. This means that over a certain time interval the perturbation locally grows. The second example is stable in the numerical computations.

In the first case the supporting interval for the perturbation is $(-15\epsilon,15\epsilon)$ (Figure 4.1), and we begin with an initial state having two peaks on both sides of zero. As time proceeds the peaks grow in the beginning, resulting in an unstable transient state. After this unstable state the solution converges to the kink solution. In the case of the supporting interval $(-3\epsilon,3\epsilon)$ in Figure 4.2, the solution converges uniformly to the kink solution without a transitional state.

Comparing the time evolution of our first two examples with the corresponding energy functionals and Willmore functionals, we can easily see differences in the graphs of functionals. We can see that in the unstable case the energy functional almost has a saddle point; in the stable case it is rapidly decreasing. Also, instabilities seem to

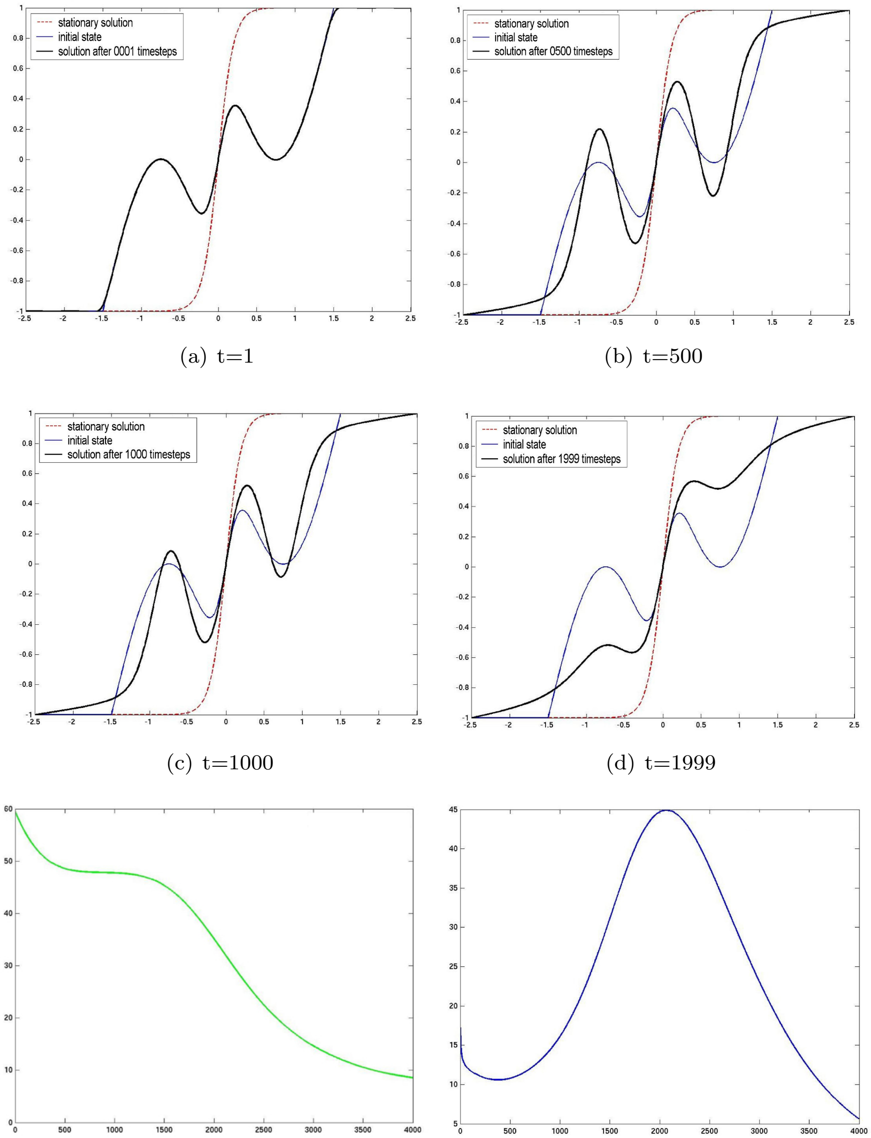

(a) t=1

(b) t=500

(c) t=1000

(d) t=1999

(e) Energy functional

(f) Willmore functional

FIG. 4.1. *(a)-(d): Evolution of the solution in time for* $\epsilon = 0.1$ *and a zero-mean perturbation supported on* $(-15\epsilon, 15\epsilon)$ *with* $a = 1$, $f = 1$ *and with corresponding energy functional (e) and Willmore functional (f)*

correspond to peaks in the graph of the Willmore functional over time. The Willmore functional increases over a finite time interval in contrast to the stable case where it decreases for all times t. Another interesting phenomenon can be seen by starting with modified versions of the perturbation p. For example we could shift the sinusoidal perturbation to the left or to the right of zero to start with an asymmetric initial state. The example in Figure 4.3 is a result of a shift of the perturbation used in

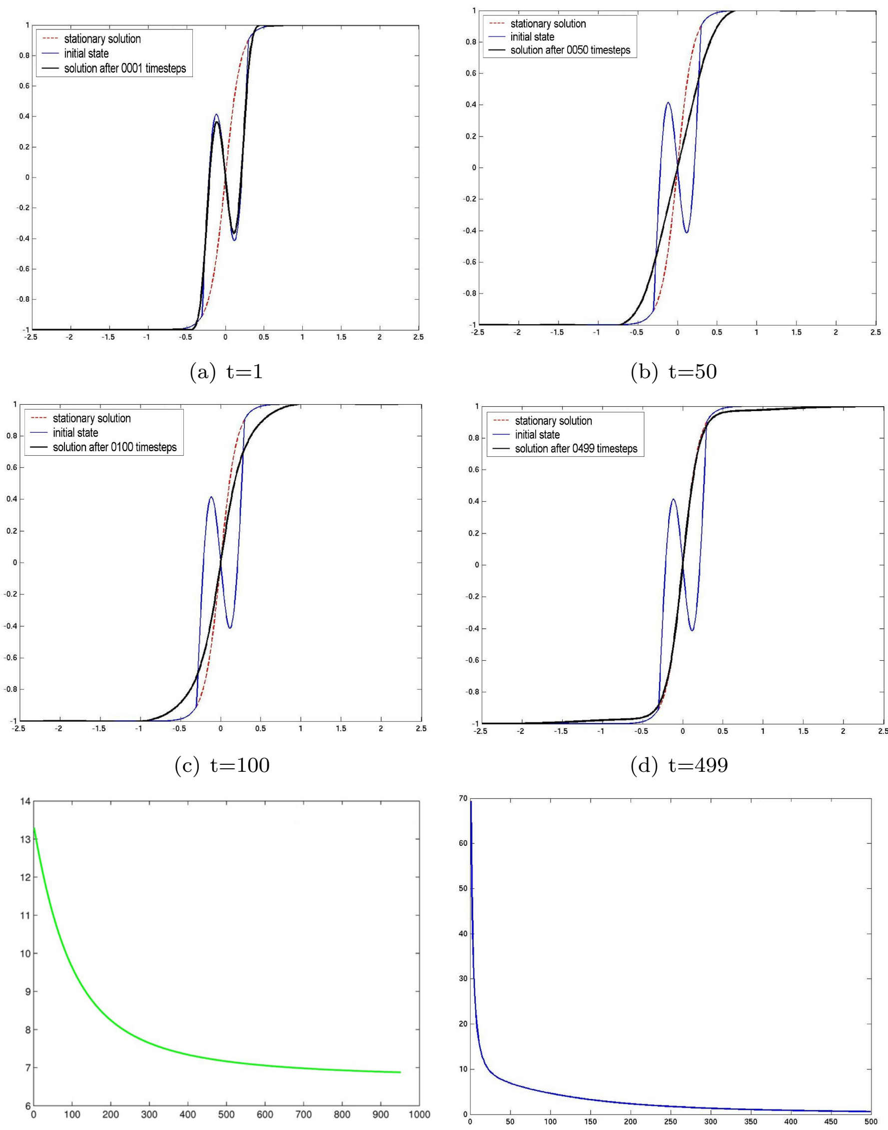

(a) t=1 (b) t=50

(c) t=100 (d) t=499

(e) Energy functional (f) Willmore functional

Fig. 4.2. *(a)-(d): Evolution of the solution in time for* $\epsilon = 0.1$ *and a zero-mean perturbation supported on* $(-3\epsilon, 3\epsilon)$ *with* $a = 1$, $f = 1$ *and with corresponding energy functional (e) and Willmore functional (f)*

the example of Figure 4.1. The shift of the perturbation leads to a shift of the kink solution asymptotically in time as a consequence of conservation of mass. Considering again the Willmore functional, an increase in time, visibly caused by a transitional instability, occurs.

Considering the behavior of the perturbed solution in several numerical tests, we can further make claims on how the perturbation has to look such that an unstable state occurs. For a fixed $\epsilon << 1$ we can see that the length of the supporting interval

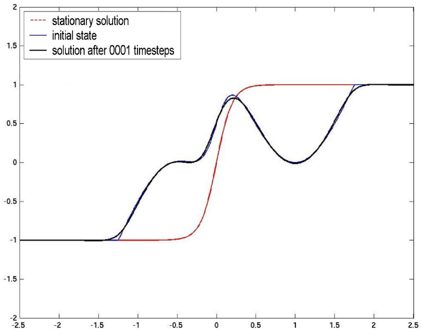

(a) t=1

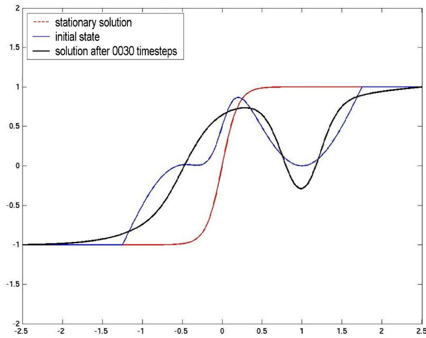

(b) t=30

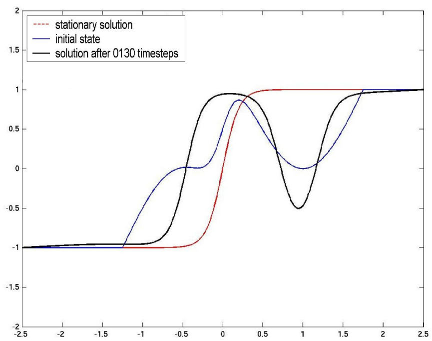

(c) t=130

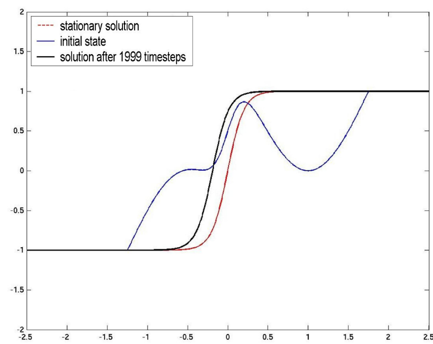

(d) t=1999

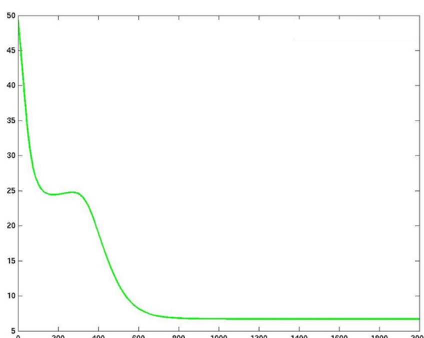

(e) Energy functional

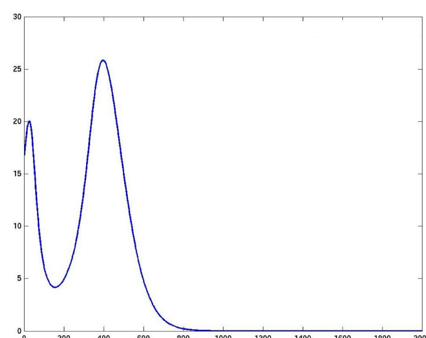

(f) Willmore functional

FIG. 4.3. *(a)-(d): Evolution of the shifted solution in time for* $\epsilon = 0.1$ *and a zero-mean perturbation supported on* $(-15\epsilon, 15\epsilon)$ *with* $a = 1$, $f = 1$ *and with corresponding energy functional (e) and Willmore functional (f)*

is most relevant. Extending the supporting interval of the perturbation brings with it an extension of the time interval and the size of the instability as a consequence; compare Figure 4.4, right diagram. If the supporting interval is too small, no unstable state can be seen; compare Figure 4.2. Also, the amplitude and the frequency of the perturbation have an influence on the occurrence and size of the instability. With growing amplitude of the perturbation, the time interval and the size of the instability change; compare Figure 4.4, left diagram. If the amplitude exceeds a certain

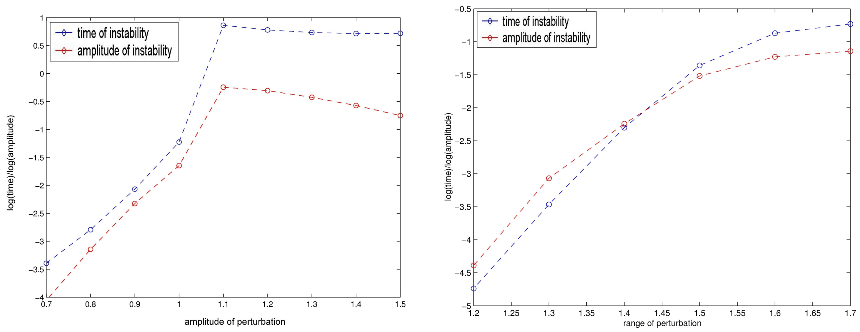

(a) (b)

Fig. 4.4. *Length of time interval and maximal amplitude of the instability for different amplitudes of the perturbation (a) and different supporting intervals of the perturbation (b).* $\epsilon = 0.1$ *fixed.*

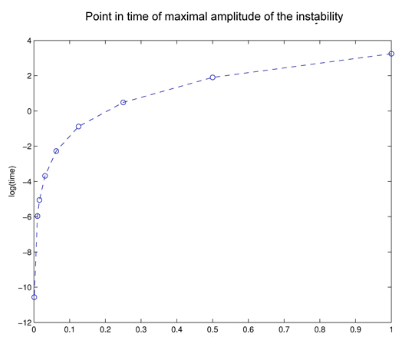

Fig. 4.5. *Length of the time interval of the instability for different values of* ϵ *for a perturbation supported on* $(-15\epsilon, 15\epsilon)$ *with* $a=1,\ f=1$.

threshold, the solution will not converge to the kink solution anymore. Furthermore, the higher the frequency of the perturbation, the faster the solution converges to the kink solution. Therefore, the higher the frequency of the perturbation, the smaller the time interval of the instability. Because of the important role of the support of the perturbation, it seems that perturbations with high frequency bring no additional information for the study of the time-local instability.

By changing the parameter ϵ, one can see that with decreasing ϵ the time interval of the instability decreases. In Figure 4.5 the point in time of the maximal amplitude of the instability is shown for different ϵ. The maximal amplitude of the instability stays approximately the same.

In the two dimensional case the analogue of the kink solutions are the so-called bubble solutions. In Figure 4.6 the evolution of a solution of the two dimensional Cahn-Hilliard equation near a bubble solution over a finite time interval is shown. In this example we used equidistant space and time discretization $\Delta x = \Delta y = \epsilon$ and $\Delta t = \epsilon^4$. As initial value we take a radial-symmetric bubble solution perturbed by a sine wave in the x_1–direction. For a better comparison with the one dimensional

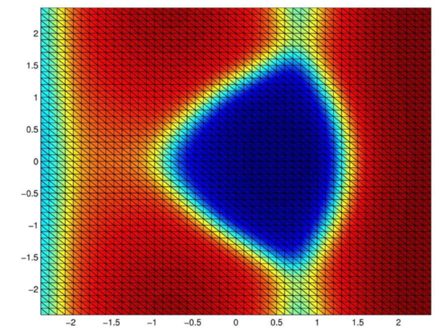

(a) t=21

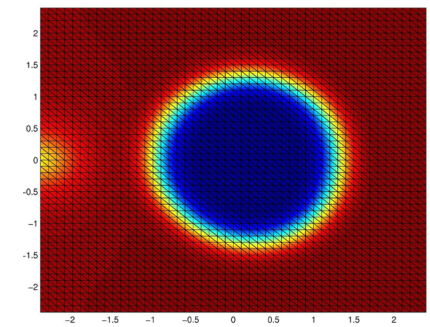

(b) t=600

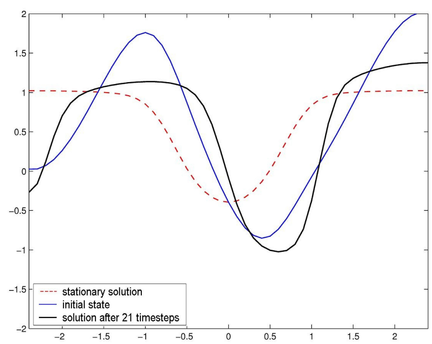

(c) t=21

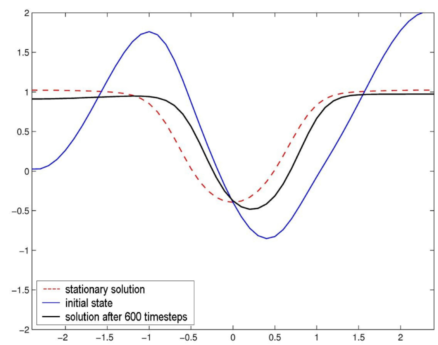

(d) t=600

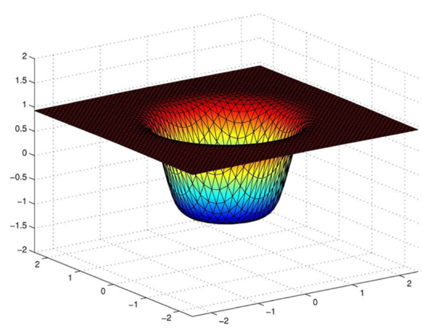

(e) Bubble solution

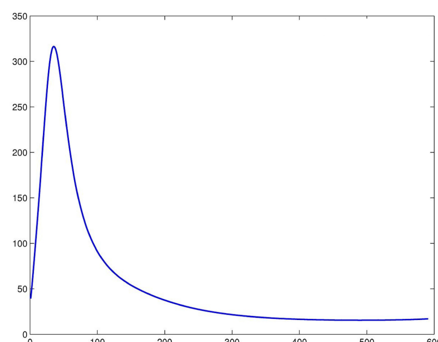

(f) Willmore functional

FIG. 4.6. *Surface plot (a)-(b) and vertical cut (c)-(d) of the solution for* $\epsilon = 0.1$ *perturbed with a sinusoidal wave in x–direction. (e) shows the bubble solution and (f) the Willmore functional*

case a vertical cut in $x_2 = 0.5$ of the solution is shown. Again the solution exhibits a local growth of amplitude before converging uniformly to the stationary solution. Especially near $x_1 = 0.5$, the solution incipiently tends away from the bubble solution. As predicted, this phenomenon causes an increase of the Willmore functional in a short time interval before it decays to 0.

5. Conclusion and outlook

We considered local instability and asymptotic behavior of the Cahn-Hilliard equation in the neighbourhood of certain transition solutions. We found that studying instabilities of the Cahn-Hilliard equation in finite time is closely connected to studying the monotonicity behavior of the Willmore functional. In Section 2 the large-time limit of the Willmore functional was shown to be zero in a general setting. With this result, the convergence of $u_t \to 0$ in $H^{-2}(\Omega)$ and in $L^2(\Omega)$ for solutions u of the Cahn-Hilliard equation in arbitrary space dimensions was also proved. The main challenge of our proof of convergence is that we avoid using the Lojasiewicz inequality, as used in previous works. The asymptotic decay rate in arbitrary dimensions is, however still a challenging problem. Further, we find that the Willmore functional is a good surveying quantity to study structures of instability patterns of the solutions. In Section 3 a formal computation for the Willmore functional, asymptotically expanded in the eigenvectors, strengthed our conjecture about the connection between the Willmore functional and the stability of solutions of the Cahn-Hilliard equation. Motivated by the linear analysis, in Section 4 local instabilities in finite time of solutions of the nonlinear Cahn-Hilliard equation near transition solutions were found numerically in one and two dimensions and compared with the behavior of the corresponding Willmore functional. We found the Willmore functional to be monotonically decreasing if the solution converges to the equilibrium state without transitional instability and having maxima when local-time instabilities occur. Therefore, the Willmore functional could be used for the mathematical and numerical analysis of the Cahn-Hilliard equation, e.g., by providing a more efficient tool for determining stability/instability of solutions. Further, it can be useful in applications of the Cahn-Hilliard equation such as in image processing (cf. [4, 5]). Therein the processed image is derived by evolving a modified Cahn-Hilliard equation until its steady state. The Willmore functional could thereby serve as a surveilling quantity reporting how far away from the steady state the solution is.

Acknowledgement. C.-B. Schönlieb acknowledges the financial support provided by the Wissenschaftskolleg (Graduiertenkolleg, Ph.D. program) of the Faculty for Mathematics at the University of Vienna, supported by the Austrian Science Fund, and of the project WWTF Five senses-Call 2006, Mathematical Methods for Image Analysis and Processing in the Visual Arts. Peter Markowich also acknowledges support from the Royal Society as Wolfson Research Merit Award Holder. We would also like to thank the referee for useful comments.

REFERENCES

[1] N. Alikakos, P.W. Bates and G. Fusco, *Slow motion for the Cahn-Hilliard equation in one space dimension*, J. Differ. Equations, 90, 1, 81–135, 1991.

[2] N. Alikakos and G. Fusco, *Slow dynamics for the Cahn-Hilliard equation in higher space dimensions. I: Spectral estimates*, Commun. Partial Differ. Equations, 19, 9-10, 1397–1447, 1994.

[3] P.W. Bates and J. Xun, *Metastable patterns for the Cahn-Hilliard equation. I.*, J. Differ. Equations, 111, 2, 421–457, 1994.

[4] A. Bertozzi, S. Esedoglu and A. Gillette, *Inpainting of binary images using the Cahn-Hilliard equation*, IEEE Trans. Image Proc., 16, 1, 285–291, 2007.

[5] A. Bertozzi, S. Esedoglu and A. Gillette, *Analysis of a two-scale Cahn-Hilliard model for image inpainting*, Multiscale Modeling and Simulation, 6, 3, 913–936, 2007.

[6] J.F. Blowey and C.M. Elliott, *The Cahn-Hilliard gradient theory for phase separation with non-smooth free energy. II: Numerical analysis*, Eur. J. Appl. Math., 3, 2, 147–179, 1992.

[7] L. Bronsard and D. Hilhorst, *On the slow dynamics for the Cahn-Hilliard equation in one space dimension*, Proc. R. Soc. Lond., Ser. A, 439, 1907, 669–682, 1992.
[8] L. Bronsard and R.V. Kohn, *On the slowness of phase boundary motion in one space dimension*, Commun. Pure Appl. Math., 43, 8, 983–997, 1990.
[9] J.W. Cahn and J.E. Hilliard, *Free energy of a non-uniform system. I. Interfacial free energy*, J. Chem. Phys., 28, 258-267, 1958.
[10] J. Carr, M.E. Gurtin and M. Slemrod, *Structured phase transitions on a finite interval*, Arch. Rat. Mech. Anal., 86, 317–351, 1984.
[11] X. Chen, *Global asymptotic limit of solutions of the Cahn-Hilliard equation*, J. Differ. Geom., 44, 2, 262–311, 1996.
[12] X. Chen and M. Kowalczyk, *Existence of equilibria for the Cahn-Hilliard equation via local minimizers of the perimeter*, Commun. Partial Differ. Equations, 21, 7-8, 1207–1233, 1996.
[13] Q. Du, C. Liu, R. Ryham and X. Wang, *A phase field formulation of the Willmore problem*, Nonlinearity, 18, 3, 1249–1267, 2005.
[14] C.M. Elliott and D.A. French, *Numerical studies of the Cahn-Hilliard equation for phase separation*, IMA J. Appl. Math., 38, 97–128, 1987.
[15] D.J. Eyre, *An unconditionally stable one-step scheme for gradient systems*, Department of Mathematics, University of Utah, Salt Lake City, 1–15, 1998.
[16] X. Feng and A. Prohl, *Error analysis of a mixed finite element method for the Cahn-Hilliard equation*, Numer. Math., 99, 1, 47–84, 2004.
[17] X. Feng and A. Prohl, *Numerical analysis of the Cahn-Hilliard equation and approximation for the Hele-Shaw problem*, Interfaces Free Bound., 7, 1, 1–28, 2005.
[18] P.C. Fife, *Models for phase separation and their mathematics*, Electronic J. Differ. Equations, 2000, 48, 1–26, 2000.
[19] P.C. Fife, H. Kielhoefer, S. Maier-Paape and T. Wanner, *Perturbation of doubly periodic solution branches with applications to the Cahn-Hilliard equation*, Physica D, 100, 1-4, 257–278, 1997.
[20] C.P. Grant, *Slow motion in one-dimensional Cahn-Morral systems*, SIAM J. Math. Anal., 26, 1, 21–34, 1995.
[21] M. Grinfeld and A. Novick-Cohen, *Counting stationary solutions of the Cahn-Hilliard equation by transversality arguments*, Proc. R. Soc. Edinb., Sect. A, 125, 2, 351–370, 1995.
[22] M. Grinfeld and A. Novick-Cohen, *The viscous Cahn-Hilliard equation: Morse decomposition and structure of the global attractor*, Trans. Am. Math. Soc., 351, 6, 2375–2406, 1999.
[23] M.E. Gurtin, *Toward a nonequilibrium thermodynamics of two-phase materials*, Arch. Rat. Mech. Anal., 100, 3, 275–312, 1988.
[24] J.K. Hale, *Asymptotic behavior of dissipative systems*, Mathematical Surveys and Monographs, A.M.S., 25, 1988.
[25] S. Łojasiewicz, *On semi- and subanalytic geometry. (Sur la géométrie semi- et sous-analytique)*, Ann. Inst. Fourier, 43, 5, 1575–1595, 1993.
[26] E.V.L. de Mello and O.T. da Silveira Filho, *Numerical study of the Cahn-Hilliard equation in one, two and three dimensions*, Physica A, 347, 429–443, 2005.
[27] B. Nicolaenko, B. Scheurer and R. Temam, *Some global dynamical properties of a class of pattern formation equations*, Commun. Partial Differ. Equations, 14, 2, 245–297, 1989.
[28] R.L. Pego, *Front migration in the nonlinear Cahn-Hilliard equation*, Proc. Roy. Soc. London Ser. A, 422, 261–278, 1989.
[29] O. Penrose and P.C. Fife, *Thermodynamically consistent models of phase-field type for the kinetics of phase transitions*, Physica D, 43, 44–62, 1990.
[30] M. Röger and R. Schätzle, *On a modified conjecture of De Giorgi*, Math. Z., 254, 4, 675–714, 2006.
[31] M. Röger and M.Y. Tonegawa, *Convergence of phase-field approximations to the Gibbs-Thomson law*, Calc. Var. Partial Differ. Equations, 2007.
[32] P. Rybka and K.H. Hoffmann, *Convergence of solutions to Cahn-Hilliard equation*, Commun. Partial Differ. Equations, 24, 5-6, 1055–1077, 1999.
[33] L. Simon, *Asymptotics for a class of non-linear evolution equations, with applications to geometric problems*, Ann. of Math., 118, 525–571, 1983.
[34] E. Sander and T. Wanner, *Unexpectedly linear behavior for the Cahn-Hilliard equation*, SIAM J. Appl. Math., 60, 6, 2182–2202, 2000.

[35] J. Wei and M. Winter, *On the stationary Cahn-Hilliard equation: Interior spike solutions*, J. Differ. Equations, 148, 2, 231–267, 1998.
[36] J. Wei and M. Winter, *On the stationary Cahn-Hilliard equation: bubble solutions*, SIAM J. Math. Anal., 29, 6, 1492–1518, 1998.
[37] J. Wei and M. Winter, *Stationary solutions for the Cahn-Hilliard equation*, Annales de l'institut Henri Poincare (C) Nonnear Analysis, 15, 4, 459–492, 1998.
[38] T.J. Willmore, *Riemannian Geometry*, Oxford Science Publications, Oxford: Clarendon Press, xi, 1993.
[39] S. Zheng, *Asymptotic behavior of solution to the Cahn-Hilliard equation*, Appl. Anal., 23, 165–184, 1986.